Research Square

Preprints are preliminary reports that have not undergone peer review.
They should not be considered conclusive, used to inform clinical practice,
or referenced by the media as validated information.

Experimental Assessment of the Fatigue Behavior of Conventional and Bio-Based Bituminous Mixtures at Different Temperatures

Sergio Hernán Manjarrés Paredes
ENTPE, Ecole Centrale de Lyon, CNRS, LTDS
Salvatore Mangiafico
salvatore.mangiafico@entpe.fr

ENTPE, Ecole Centrale de Lyon, CNRS, LTDS
Cédric Sauzéat
ENTPE, Ecole Centrale de Lyon, CNRS, LTDS
Julien Van Rompu
Eiffage Route
Vincent Le Menec
Eiffage Route

Research Article

Keywords: Fatigue behavior, Bio-based bituminous mixtures, Temperature effects, Storage time, 2PB tests, Tension/compression tests

Posted Date: November 20th, 2026

DOI: https://doi.org/10.21203/rs.3.rs-11394331/v1

License: This work is licensed under a Creative Commons Attribution 4.0 International License.
Read Full License

Additional Declarations: No competing interests reported.

Experimental Assessment of the Fatigue Behavior of Conventional and Bio-Based Bituminous Mixtures at Different Temperatures

Sergio Hernán Manjarrés Paredes[1] · Salvatore Mangiafico[1] · Cédric Sauzéat[1] · Julien Van Rompu[2] · Vincent le Menec[3]

[1] ENTPE, Ecole Centrale de Lyon, CNRS, LTDS, UMR5513, 69518 Vaulx-en-Velin, France
[2] Eiffage Route, 69964 Corbas, France
[3] Eiffage Route, 02220 Ciry-Salsogne, France

Corresponding author

Salvatore Mangiafico, salvatore.mangiafico@entpe.fr

ORCID

Sergio Hernán Manjarrés Paredes: [0000-0001-7721-7572], Salvatore Mangiafico: [0000-0003-0548-6989], Cédric Sauzéat: [0000-0001-5055-8887], Julien Van Rompu: [0000-0003-3920-1910]

Abstract

This study investigates the fatigue behavior of a conventional bituminous mixture (Hot 70/100) and a bio-based mixture (Warm Bio), focusing on temperature, strain amplitude, test configuration, saturation conditioning, and storage time between fabrication and testing. A total of 205 specimens were tested under cyclic loading using two-point bending (2PB) and tension/compression (T/C) configurations, under displacement control and strain control, respectively. Fatigue behavior was evaluated through the evolution of thermomechanical parameters, Wöhler curves, and the fatigue parameters (ε_6) and (1/b). Additional 2PB tests at 10 °C investigated saturation conditioning and storage times of up to 12 months.

The effect of temperature on fatigue resistance was found to be strongly dependent of the material. Hot 70/100 generally exhibited longer fatigue lives and higher (ε_6) values with increasing temperature, whereas Warm Bio showed no consistent temperature-related improvement. T/C tests yielded substantially lower (ε_6) values than 2PB tests, while Wöhler curve slopes remained comparable. Saturation conditioning had no relevant effect on Hot 70/100. For Warm Bio, the apparent improvement after saturation could not be separated from the potential effect of longer storage time of specimens before testing. Warm Bio showed a marked time-dependent evolution, with increasing initial modulus, decreasing phase angle, and longer fatigue life.

These results show that fatigue trends established for conventional mixtures cannot be directly transferred to bio-based mixtures and that specimen storage and testing timelines must be carefully controlled.

Keywords: Fatigue behavior; Bio-based bituminous mixtures; Temperature effects; Storage time; 2PB tests; Tension/compression tests.

1. Introduction

Fatigue cracking is one of the principal deterioration mechanisms affecting asphalt pavements under repeated traffic loading [1]. The fatigue response of bituminous mixtures is highly sensitive to both loading conditions and temperature [1-3]. The influence of loading conditions and temperature on fatigue behavior has been investigated using various experimental approaches [1,3,5]. Under strain-controlled cyclic loading at a fixed loading frequency, increasing temperature generally reduces the initial stiffness and increase the phase angle, thereby modifying the stress response at a given strain amplitude [4]. At a given temperature and frequency, increasing the imposed strain amplitude generally shortens fatigue life [3]. Fatigue life is commonly described using Wöhler relationships linking the imposed strain amplitude to the number of cycles to failure under specified test conditions. Accordingly, temperature and strain level must be carefully considered when assessing fatigue performance and, particularly, when comparing results obtained under different testing conditions [1,5].

Fatigue characterization is also strongly influenced by the experimental procedures used to generate and interpret the measured response. Differences in test configuration can lead to different fatigue life even for the same material [1, 6]. Loading frequency is an additional protocol variable that must be considered when comparing results. These considerations are particularly relevant when comparing two-point bending (2PB) and tension/compression (T/C) tests. In 2PB, the reported strain amplitude is a nominal maximum calculated from the imposed displacement and specimen geometry within a nonuniform strain field and derived from elastic beam theory [7]. In T/C configuration, axial strain is measured over a central gauge length, where the strain field can be considered homogeneous before detectable damage localization [6,8]. Fatigue life estimation also depends on the selected failure criterion. The conventional criterion based on a 50% reduction in the initial complex modulus magnitude is widely used but it does not necessarily identify the transition from the approximately linear decrease in modulus during Phase II to the accelerated degradation in Phase III [8,9]. Alternative criteria based on phase-angle evolution, dissipated energy, or changes in measured mechanical parameters have therefore been proposed to relate fatigue failure to changes in the specimen response and damage localization [8,9]. Consequently, comparisons between fatigue results obtained using different configurations or failure criteria require careful consideration of both the loading conditions and the physical meaning of the selected criterion.

In parallel with efforts to improve pavement durability, the road industry is exploring alternatives to reduce dependence on fossil resources and the environmental impacts of asphalt production [10,11]. Bio-based binders have received growing attention as partial or full substitutes for petroleum-derived bitumen, offering opportunities to incorporate renewable resources and potentially reduce greenhouse gas emissions [10,12]. These binders can also be combined with warm-mix technologies and reclaimed asphalt pavement (RAP) to reduce production temperatures and virgin material demand [11]. However, the environmental benefits depend on the specific production system and the scope of the life cycle assessment [12]. The term bio-binder includes materials derived from diverse biomass sources and conversion processes, with correspondingly different rheological and mechanical properties [10]. Performance reported for a particular bio-based binder or mixture should therefore not be generalized without considering its composition and processing history. Blending with aged RAP binder [13], evolution of properties during aging [14] and long-term mechanical performance [10,16] consequently require further analysis.

Despite the growing body of research on bio-based binders and mixtures, their fatigue performance still deserves further attention. Studies on mixtures containing wood-derived bio-oil and lignin have reported differing fatigue responses relative to conventional mixtures, highlighting the importance of composition, aging condition, and evaluation method [15,16]. Recent investigations of mixtures containing tall oil pitch also indicate that the apparent differences in their behavior from conventional materials can depend on the applied strain level [17]. These findings emphasize the need to account for material history and testing conditions when interpreting fatigue results. However, laboratory aging studies do not directly establish how fatigue performance evolves during the interval between fabrication and testing under ambient storage conditions. Further experimental work is therefore needed to distinguish the influence of specimen age from that of test temperature, configuration, and conditioning. This distinction is particularly relevant when conditioning procedures or separate test campaigns involve specimens tested at different ages, because any evolution during storage could contribute to the measured differences. Explicitly treating storage time after fabrication as an experimental variable would help assess whether such differences arise from the investigated factor, changes in the material over time, or both.

The objective of this study is to provide a comprehensive experimental comparison of the fatigue behavior of a conventional bituminous mixture and an alternative mixture containing bio-binder. The investigation considers the combined influence of temperature and strain amplitude, and also compares results obtained using two-point bending (2PB) and tension/compression (T/C) configurations. Additional analyses address the effect of a saturation protocol and, importantly, the storage time between mixture fabrication and fatigue testing. By considering these variables within the same experimental framework, the study aims not only to compare the fatigue resistance of the two materials, but also to identify the extent to which testing conditions and material history influence the interpretation of their mechanical response. Particular attention is therefore given to whether the fatigue behavior of the bio-binder mixture can be interpreted using trends established for conventional materials, and to the role of specimen history as an additional experimental variable when characterizing emerging bio-based pavement materials.

2. Materials and methods

2.1 Materials

Two GB3-type bituminous mixtures intended for base-course applications were investigated. The reference mixture, denoted Hot 70/100, was produced as a conventional hot-mix asphalt using a 70/100 penetration-grade bitumen. The second mixture, denoted Warm Bio, incorporated a bio-binder and was manufactured at a reduced temperature. Both materials were produced at the Eiffage CERF research facility in Ciry-Salsogne, France.

The mixtures were formulated to maintain comparable characteristics. Both mixtures had the same 0/14 mm aggregate gradation (Fig. 1), contained 40% reclaimed asphalt pavement (RAP, 0/10 mm), and had a total binder content of 4.6% by mass of the mixture, including both virgin and RAP binder. The main differences therefore concerned the type of added binder and the mixing and compaction temperatures. The main mixture and binder characteristics are summarized in Table 1.

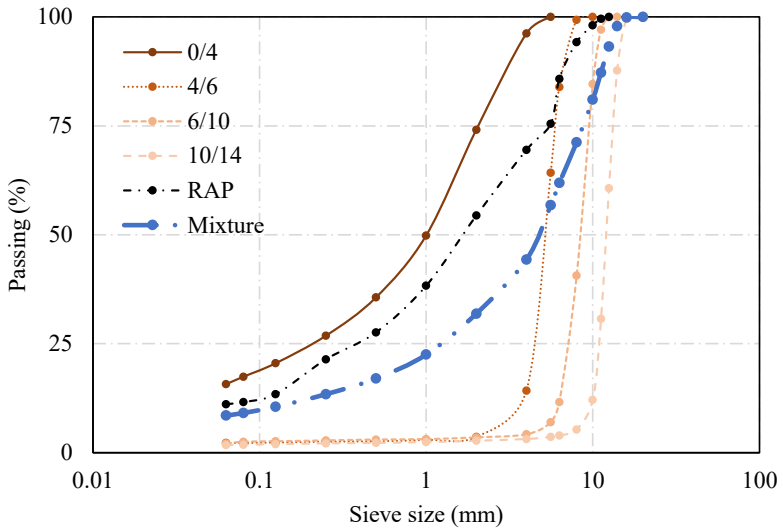


Fig. 1. Aggregate gradation curve for both mixtures.

Table 1. Main composition, production conditions and binder properties of the investigated mixtures.

Parameters/properties	Unit	Hot 70/100	Warm Bio
Mixture main composition (kept constant)			
Gradation	-	0/14	0/14
RAP content	wt%	40	40
Binder content	wt%	4.6	4.6
Target void content	%	7-8	7-8
Mixture binder and compaction temperature (intentionally varied)			
Binder	-	70/100	Bio-binder
Mixing temperature	°C	165°C	130°C
Binder properties			
Penetration grade, neat binder	0.1 mm	75	99
Softening point, neat binder	°C	46.2	89.0
Softening point, RAP-binder	°C	73.8	73.8

The mixtures were prepared in accordance with NF EN 12697-35 [18] using a laboratory twin-shaft horizontal mixer. After preheating and weighing the constituents, the aggregates were dry-mixed for 15 s, followed by the addition of RAP and a further 30 s of mixing. The binder was then introduced and the complete mixture was mixed for 2 min. The target mixing temperatures were 175 °C for Hot 70/100 and 145 °C for Warm Bio, with binder preheating temperatures of 145 and 130 °C, respectively.

Immediately after mixing, the mixtures were compacted in accordance with NF EN 12697-33+A1[19] using a pneumatic roller compactor. Slabs measuring 600 × 400 × 130 mm were produced at target compaction temperatures of 165 °C for Hot 70/100 and 130 °C for Warm Bio. Both mixtures had the same measured density of 2.513 Mg/m³ and a target air-void content of 7.5%. Hot 70/100 was compacted at 165°C, whereas Warm Bio at 130°C.

Two specimen geometries were used for fatigue testing: cylindrical and trapezoidal specimens. Cylindrical specimens were cored to a diameter of 75 mm and a height of 150 mm, whereas trapezoidal

specimens were prepared in accordance with the geometric requirements of NF EN 12697-24 [20]. Only specimens with an air-void content within ±1.5 percentage points of the target value were retained for testing.

2.2 Experimental program

The experimental program was designed to compare the fatigue behavior of the two investigated mixtures, Hot 70/100 and Warm Bio, using two testing configurations: tension/compression (TC) and two-point bending (2PB).

For the TC configuration, continuous-loading fatigue tests were performed at 10 and 20 °C for both mixtures. An additional temperature of 30 °C was investigated for Hot 70/100 in order to extend the temperature range considered for the conventional mixture.

For the 2PB configuration, continuous-loading fatigue tests were conducted at 10, 15 and 20 °C for both Hot 70/100 and Warm Bio. Additional 2PB tests at 10 °C were used to investigate the influence of the saturation protocol and storage time between mixture fabrication and fatigue testing. The experimental program, including the investigated materials, test configurations, temperatures, and additional conditioning, is summarized in Fig. 2.

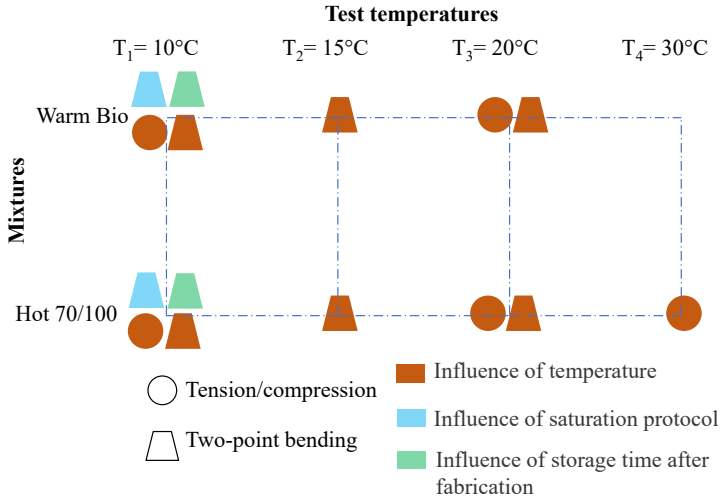


Fig. 2. Schematic representation of the experimental program.

The experimental program used for the fatigue characterization is summarized in Table 2. For each test configuration and experimental condition, the table reports the investigated strain levels, the total number of specimens, the number of replicates tested at each strain level, and the storage time between mixture fabrication and testing. These storage time differences are particularly important because they constitute a key experimental variable in the interpretation of the mechanical response for Warm Bio. They are therefore reported explicitly and considered when comparing the fatigue performance of the investigated mixtures.

Table 2. Experimental program for the fatigue testing, including test configuration, strain levels, and number of specimens.

Material	Test configuration	Test temperature - Conditioning	Target strain level (µm/m)	Specimens	Specimens per strain level	Total Storage time (Days)
Hot 70/100	2PB	10°C	100, 130, 160	18	6	30 to 50
		10°C - Saturation protocol	100, 130, 160	18	6	307 to 323
		10°C - Storage times (3, 6, 12 months)	92	18	18 (6 per storage time)	98 to 110 178 to 188 355 to 365
		15°C	110, 140, 170	18	6	35 to 43
		20°C	100, 120, 150	18	6	15 to 65
	T/C	10°C	65 to 100	5	1	562 to 599
		20°C	80 to 120	5	1	661 to 704
		30°C	100 to 155	5	1	763 to 780
Warm Bio	2PB	10°C	70, 100, 130	18	6	16 to 35
		10°C - Saturation protocol	100, 120, 140	18	6	333 to 366
		10°C - Storage times (3, 6, 12 months)	109	18	18 (6 per storage time)	111 to 114 189 to 201 366 to 370
		15°C	60, 80, 100	18	6	30 to 50
		20°C	70, 100, 130	18	6	33 to 50
	T/C	10°C	65 to 100	5	1	436 to 468
		20°C	45 to 100	5	1	475 to 525

2.3 Sample conditioning

Prior to fatigue testing, all specimens were stored for a minimum of two weeks at ambient temperature. During this period, they were kept horizontally on a sand bed and protected from direct sunlight and rain. Only 2PB specimens were specifically retained for the additional investigations of the saturation protocol and the influence of storage time between mixture fabrication and fatigue testing.

The saturation procedure was adapted from the vacuum saturation principle used in EN 12697-12 [22]. Specimens were placed in a vacuum desiccator and subjected to an absolute pressure of 8 kPa for approximately 15 min to remove entrapped air. Water was then introduced while maintaining the vacuum, and the specimens were kept fully submerged at 8 kPa for 24 h. The pressure was subsequently returned gradually to atmospheric conditions, after which the specimens remained immersed for an additional 30 min.

Prior to fatigue testing, the saturated specimens were vacuum-dried at an absolute pressure of 8 kPa for 7 days. This drying stage was introduced to remove absorbed water without thermal conditioning and to avoid progressive changes in moisture content during the long-duration fatigue tests, which could otherwise interfere with the interpretation of the fatigue response.

For the storage time investigation, all specimens were first sawn to their final dimensions and allowed to stabilize for two weeks before their dimensions and mass were recorded. The specimens were then assigned to the different storage groups and kept horizontally on a sand bed inside a thermal chamber maintained at 18 °C. Fatigue testing was subsequently performed after storage times of 3, 6, and 12 months following mixture fabrication.

Before cyclic loading, all specimens were placed in the climatic chamber and fully instrumented for 4 h at the target test temperature. This conditioning period was used to ensure a homogeneous temperature throughout the specimen before the start of the fatigue test.

2.4 Experimental methods

2.4.1 Two-point bending tests

The two-point bending fatigue tests were conducted on trapezoidal specimens in accordance with EN 12697-24 [20] using two automated two-point bending testing systems, at constant temperature and a loading frequency of 25 Hz. Prior to cyclic loading, the specimens were conditioned in the thermal chamber for 4 h to ensure thermal equilibrium. The head-displacement amplitude was then adjusted using the testing system to obtain the target strain amplitude, defined as the maximum strain in the specimen. The test was terminated when the force amplitude decreased to 5% of its initial value, taken as the force amplitude measured at the 100th loading cycle.

The measured peaks of the sinusoidal signals of the force, (F), and head displacement, (Z), were used to determine the real and imaginary parts of the complex modulus, (E_1) and (E_2), respectively. The magnitude of the complex modulus, (|E*|), was then calculated from these two components according to Eq. 1, Eq. 2 and Eq. 3 :

$$E_1 = \gamma\left(\frac{F}{Z}\cos(\varphi) + 10^{-6} \times \mu\omega^2\right) \quad \textbf{Eq. 1}$$

$$E_2 = \gamma\frac{F}{Z}\sin(\varphi) \quad \textbf{Eq. 2}$$

$$|E^*| = \sqrt{E_1^2 + E_2^2} \quad \textbf{Eq. 3}$$

where, γ is a form factor depending on the sample geometry in mm^{-1}, μ is a mass factor in g. The obtention of these values is shown in Eq. 4 and Eq. 5.

$$\gamma = \frac{12L^3}{b(h_1 - h_2)^3}\left[\left(2 - \frac{h_2}{2h_1}\right)\frac{h_2}{h_1} - \frac{3}{2} - \ln\frac{h_2}{h_1}\right] \quad \textbf{Eq. 4}$$

$$\mu = 0.135M + m \quad \textbf{Eq. 5}$$

The maximum strain is therefore calculated using the relationships defined in EN 12697-26+A1 [21], which are derived from elastic beam theory. These relationships allow both the location of the maximum tensile strain within the specimen and its magnitude (Eq. 6 and Eq. 7) to be determined.

$$Max(\varepsilon_{11}) = K_\varepsilon \times Z \quad \textbf{Eq. 6}$$

$$K_\varepsilon = \frac{B^2 \times (B-b)^2}{4hb[(b-B) \times (3B-b) + 2B^2 \times ln\left(\frac{B}{b}\right)} \quad \textbf{Eq. 7}$$

2.4.2 Tension/compression tests

Tension/compression tests were performed on cylindrical specimens under strain-controlled axial sinusoidal loading using a servo-hydraulic testing system. Axial strain was measured with three extensometers positioned at 120° intervals around the specimen mid-height, while radial strain was monitored in two orthogonal directions using four non-contact displacement sensors. By convention, Direction 1 was defined as the axial direction, Direction 2 as the slab compaction direction, and Direction 3 as the remaining principal direction, orthogonal to Directions 1 and 2. Specimen temperature was continuously recorded with

a PT100 temperature sensor attached to the specimen surface. The experimental setup and specimen instrumentation are shown in Fig. 3.

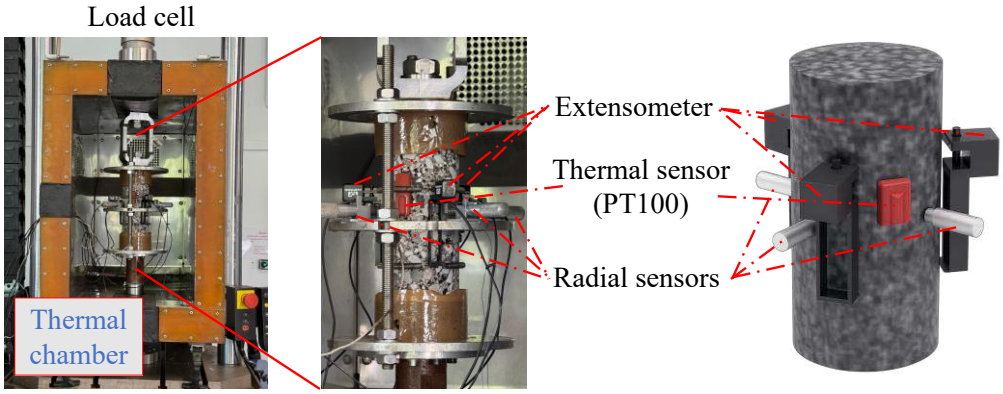


Fig. 3. Experimental set-up used for tension/compression (T/C) tests

The tension/compression fatigue tests were conducted on cylindrical specimens at constant temperature, using a loading frequency of 10 Hz and a single target strain amplitude for each tested specimen. Prior to cyclic loading, the specimens were conditioned in the thermal chamber for 4 h. During this period, a compressive force of 0.03 kN was maintained for tests at 10 and 20 °C, whereas zero strain was maintained under strain control for tests at 30 °C. The specimens were then subjected to sinusoidal loading under strain-controlled conditions.

The test was terminated when any of the following limits was reached: a change in actuator displacement greater than ±2.5 mm from its initial position, a measured force exceeding ±18 kN, or an extensometer displacement exceeding ±0.9 mm. These limits were used solely to define the end of the test and do not correspond to the fatigue failure criteria used for data analysis.

The imposed axial strain, (ε), was defined as the average strain measured by the three extensometers (Eq. 8), with strain amplitude (ε_0) and angular frequency (ω). Since the tension/compression configuration provides a homogeneous stress and strain field within the instrumented central region of the specimen, the axial strain and stress can be obtained directly from the measured displacements and applied force, respectively. The corresponding stress response, (σ), with amplitude (σ_0), was calculated from the force measured by the load cell and is expressed in Eq. 9.

For each loading cycle, the complex modulus, (E*), was determined according to Eq. 10, where ($|E^*|$) represents its norm and (φ_E) its phase angle (the phase difference between the stress and axial strain signals).

$$\varepsilon(t) = \varepsilon_0 \sin(\omega t - \varphi_E) \quad \textbf{Eq. 8}$$

$$\sigma(t) = \sigma_0 \sin(\omega t) \quad \textbf{Eq. 9}$$

$$E^* = \frac{\sigma_0}{\varepsilon_0} e^{i\varphi_E} = |E^*| e^{i\varphi_E} \quad \textbf{Eq. 10}$$

The complex Poisson's ratio, (ν^*), was determined from the ratio between the radial strain, (ε_r), and the axial strain, (ε), as expressed in Eq. 11 and Eq. 12 for Direction 2 and Eq. 13 and Eq. 14 for Direction 3:

$$\varepsilon_{r2}(t) = \varepsilon_{r20} \sin(\omega t - \varphi_E + \pi + \varphi_{\nu 2}) \quad \textbf{Eq. 11}$$

$$\nu_2{}^* = \frac{\varepsilon_{r20}}{\varepsilon_0} e^{i\varphi_{\nu 2}} = |\nu_2{}^*| e^{i\varphi_{\nu 2}} \quad \textbf{Eq. 12}$$

$$\varepsilon_{r3}(t) = \varepsilon_{r30} \sin(\omega t - \varphi_E + \pi + \varphi_{v3}) \quad \textbf{Eq. 13}$$

$$\nu_3{}^* = \frac{\varepsilon_{r30}}{\varepsilon_0} e^{i\varphi_{v3}} = |\nu_3{}^*| e^{i\varphi_{v3}} \quad \textbf{Eq. 14}$$

where (|ν*|) is the norm of the complex Poisson's ratio and (φ_v) is its phase angle (the phase difference associated with the relationship between the radial strain and axial strain signals).

For the determination of complex modulus, the amplitudes and phase shifts of stress and strain signals were obtained by least-squares fitting with sinusoidal functions.

The mean strain values were retained because they provide information on the progressive change in specimen dimensions during fatigue loading. In particular, the mean axial and radial strains were used to calculate the mean volumetric strain and to evaluate the dilation or contraction of the specimen.

The volumetric strain was calculated from the axial and radial strain measurements assuming small strain conditions. It is defined as the sum of the three principal normal strain components (Eq. 15). For cylindrical specimens in uniaxial loading, the expression becomes Eq. 16. And the signal is presented in Eq. 17. The volumetric strain signal was decomposed into a mean component, ($\overline{\varepsilon_{vol}}$), representing the net volumetric dilation or contraction of the specimen, and an oscillatory component of amplitude (ε_{vol0}) and phase angle (φ_{vol}) the phase of the volumetric strain signal relative to the chosen temporal reference; in the present formulation, this reference is linked to the stress signal through (φ_E).

$$\varepsilon_{vol} = \varepsilon_1 + \varepsilon_2 + \varepsilon_3 \quad \textbf{Eq. 15}$$

$$\varepsilon_{vol} = \varepsilon + \varepsilon_{r2} + \varepsilon_{r3} \quad \textbf{Eq. 16}$$

$$\varepsilon_{vol}(t) = \overline{\varepsilon_{vol}} + \varepsilon_{vol0} \sin(\omega t - \varphi_{vol}) \quad \textbf{Eq. 17}$$

2.5 Fatigue failure criteria used in the study

The DER criterion adopted in this work is based on the evolution of the dissipated energy ratio (Eq. 19) and identifies failure from a change in the slope of the DER–cycle relationship (Fig. 4a). A reference slope was first obtained by linear regression over the interval from 5,000 to 15,000 cycles. The upper limit of the regression interval was then progressively extended in increments of 10,000 cycles, while the lower limit remained fixed at 5,000 cycles. A new slope was calculated for each extended interval. The criterion was reached when the absolute value of the regression slope increased by 20% relative to the reference slope. The associated number of cycles, ($N_{f\ DER}$), was determined by linear interpolation between the two consecutive regression intervals surrounding the 20% threshold. The dissipated energy per cycle per unit volume was calculated using Eq. 19

$$DER = \frac{\sum_{i=1}^{N} W_i}{W_N} \quad \textbf{Eq. 18}$$

$$W_{cycle} = \pi\, \sigma_0\, \varepsilon_0\, sin\, \varphi_E \quad \textbf{Eq. 19}$$

Where N is the considered cycle and W_N is the energy dissipated during the considered cycle.

The dissipated energy ratio (DER) criterion was retained to evaluate fatigue life in both 2PB and T/C tests. The conventional 50% reduction in initial |E*| did not consistently identify the transition from Phase II to Phase III [3,8], sometimes indicating failure while the response clearly entered to Phase III. An energy-based criterion [9] was therefore selected to analyze both mixtures across the investigated temperatures. Nevertheless, DER criterion interpretation is more straightforward in T/C tests, where

approximately homogeneous stress and strain fields develop within the instrumented region. In 2PB tests, these fields are non-uniform, so energy dissipation varies throughout the specimen. Applying the same criterion provides a common basis for analysis, although it does not eliminate the differences between the two test configurations.

An example of DER analysis is presented in Fig. 4 for Hot 70/100 tested at 30°C and 100 µm/m in tension/compression configuration.

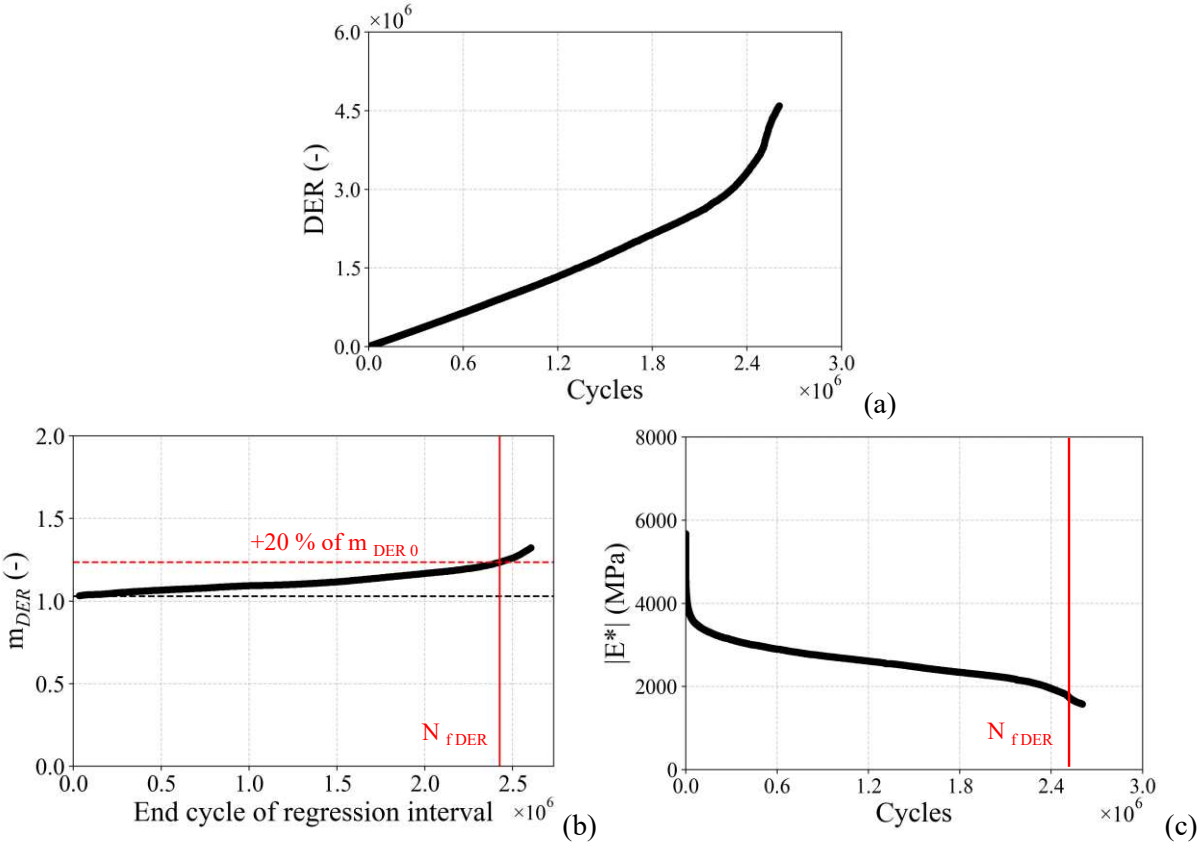


Fig. 4. DER failure criterion, 30°C – 100 µm/m in T/C tests for Hot 70/100: (a) DER vs cycles, (b) slope of DER, (c) $N_{f\,DER}$ in the norm of the complex modulus vs cycles

3. Experimental results and analysis

3.1 Influence of test temperature

3.1.1 Comparison of 2PB fatigue test results at different temperatures and same equivalent strain level (100 µm/m)

As a first step, the fatigue response observed at a common strain amplitude of 100 µm/m for different samples of the two materials at different temperatures was compared. The 2PB configuration was selected for this comparison because a larger number of replicate specimens was tested at the same strain level, providing a more robust basis for evaluating the effect of temperature under equivalent loading conditions. Hot 70/100 was analyzed at 10°C and 20°C, Warm Bio at 10°C, 15°C, and 20°C.

Fig. 5 shows the evolution of the norm and phase angle of complex modulus and the dissipated energy with the number of loading cycles for Hot 70/100 tested in the 2PB configuration at a strain amplitude of 100 µm/m.

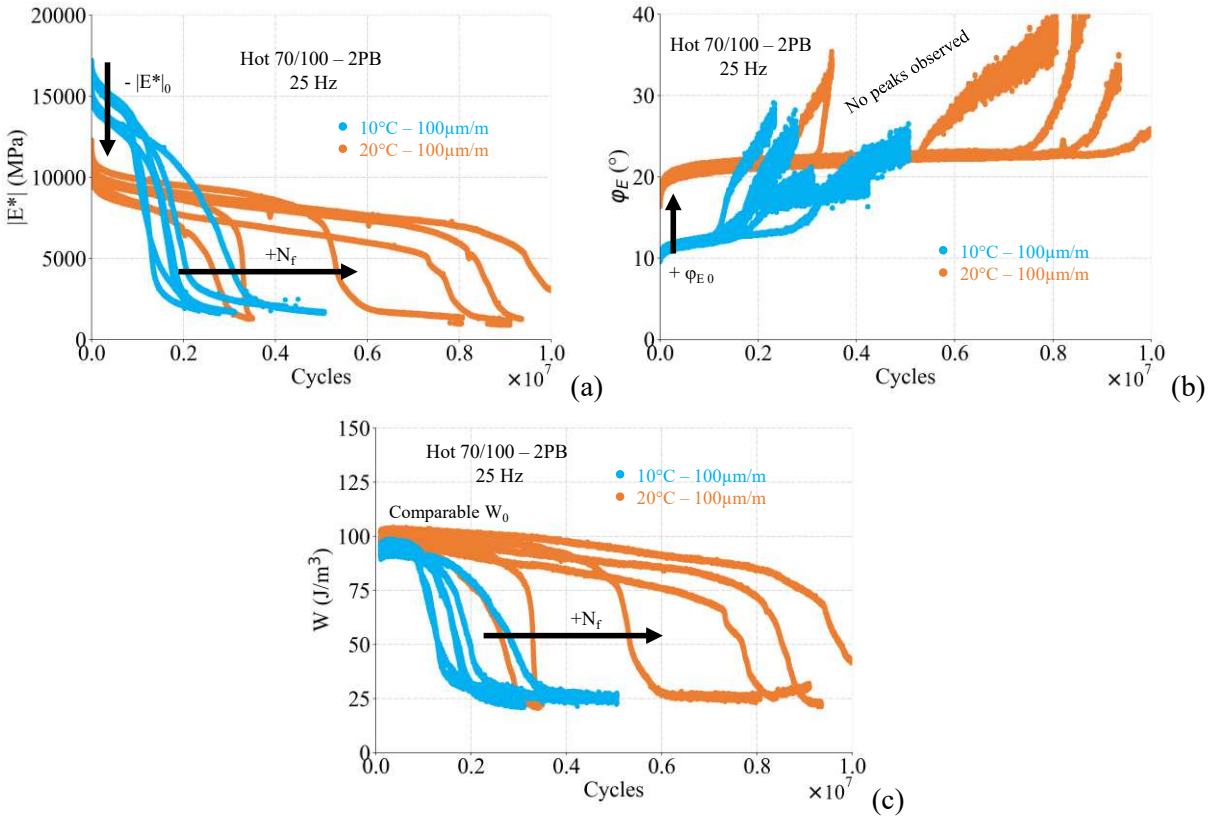


Fig. 5. Comparison of Hot 70/100 specimens tested in 2PB at 100 µm/m and at 10 and 20°C: evolution with the number of loading cycles of norm (a) and phase angle (b) of complex modulus and dissipated energy per cycle (c).

As shown in Fig. 5a, the initial norm of the complex modulus decreases with increasing temperature. During Phase II, the relative reduction in (|E*|) with loading cycles is slower at 20 °C than at 10 °C. Moreover, specimens tested at 20 °C withstand a greater number of loading cycles at the same strain amplitude, indicating improved fatigue resistance at the higher temperature. The longer fatigue life observed at the higher temperature is consistent with trends reported for other bituminous mixtures under strain-controlled loading, although this dependence may change over a wider temperature range [3,5]. The initial phase angle is also higher at 20 °C, as shown in Fig. 5b, whereas its evolution during Phase II is similar at both temperatures.

The dissipated energy evolution is presented in Fig. 5c. Since the dissipated energy per cycle depends on both the norm and phase angle of the complex modulus, its evolution reflects the combined effect of these parameters. In this case, the reduction in |E*| associated with increasing temperature is partly compensated by the corresponding increase in phase angle, resulting in dissipated energy levels of a comparable order of magnitude at both temperatures.

Fig. 6 shows the evolution of the norm and phase angle of the complex modulus and the dissipated energy with the number of loading cycles for Warm Bio tested in the 2PB configuration at a strain amplitude of 100 µm/m. Tests were conducted at 10, 15, and 20 °C, with six specimens tested at each temperature.

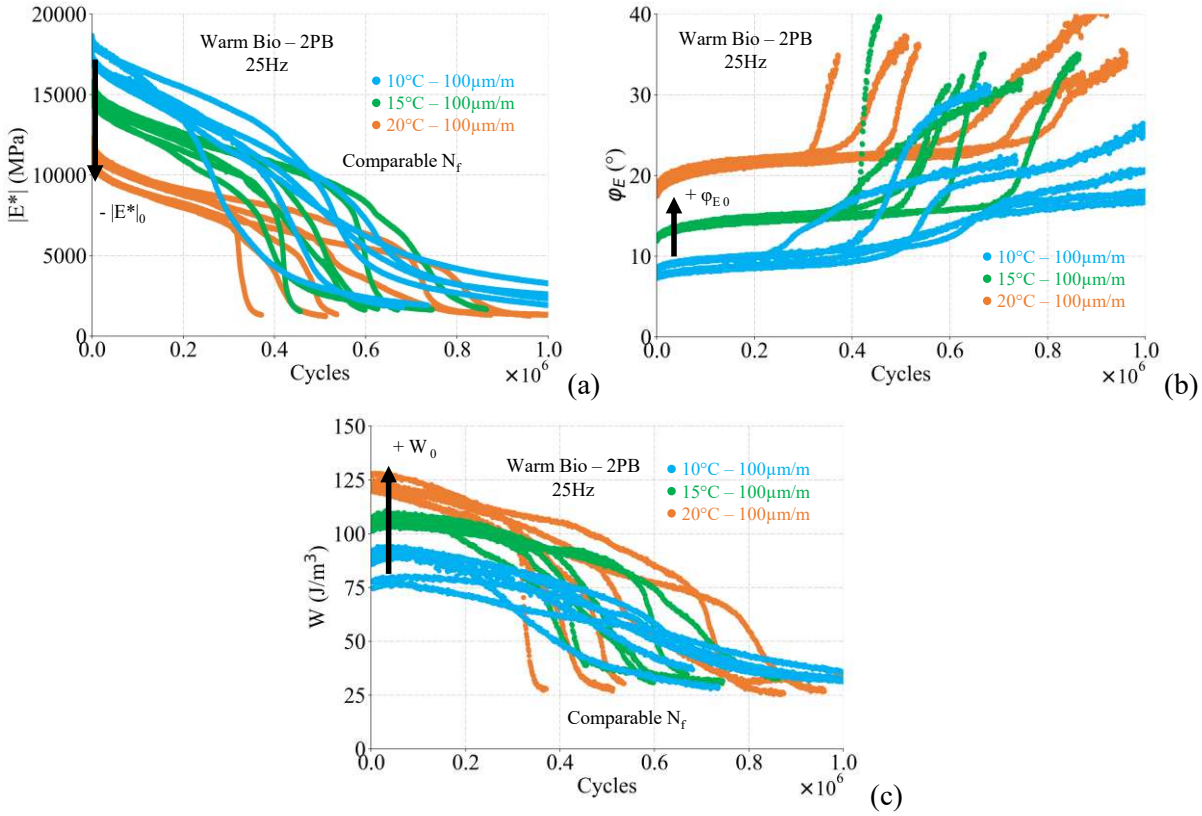


Fig. 6. Comparison of Warm Bio specimens tested in 2PB at 100 µm/m and at 10 and 20°C: evolution with the number of loading cycles of norm(a) and (b) phase angle of the complex modulus, and the dissipated energy (c).

As shown in Fig. 6a, the initial norm of the complex modulus decreases as temperature increases. However, unlike Hot 70/100, no clear increase in fatigue life is observed over the investigated temperature range. At 100 µm/m, the fatigue lives obtained at 10°C, 15°C, and 20°C are of a comparable order of magnitude, indicating no systematic temperature-related improvement in fatigue resistance.

The initial phase angle (φ_E) increases with temperature, as shown in Fig. 6b. The dissipated energy per cycle (W_0) also increases with temperature (Fig. 6c). In this case, the increase in phase angle appears to outweigh the reduction in the norm of the complex modulus, resulting in higher dissipated energy levels at higher temperatures.

3.1.2 Comparison of T/C fatigue test results at different temperatures and strain levels

The combined influence of temperature and strain amplitude was evaluated using the T/C configuration, since a larger number of strain levels was investigated with this setup. Hot 70/100 was tested at 10°C, 20°C, and 30°C, whereas Warm Bio was tested at 10°C and 20°C. For each temperature, five strain amplitudes were considered, with one specimen tested at each strain level.

Fig. 7 presents the evolution of the norm and phase angle of the complex modulus and the dissipated energy with the number of loading cycles for the investigated T/C conditions, for Hot 70/100.

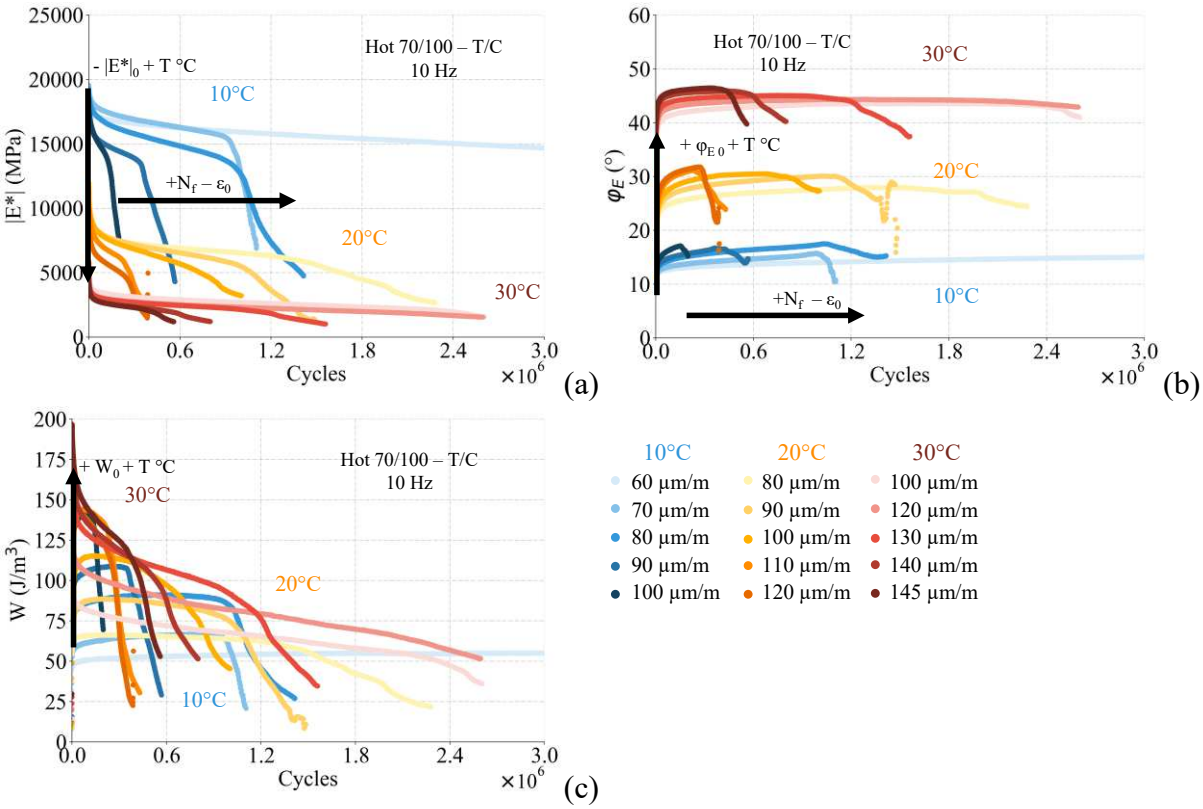


Fig. 7. Comparison of Hot 70/100 specimens tested in T/C at different strain levels at 10, 20 and 30°C: evolution with the number of loading cycles of norm (a) and phase angle (b) of complex modulus and dissipated energy per cycle (c).

Fig. 7a shows the expected influence of temperature on the initial norm of the complex modulus. The effect of strain amplitude effect is also observed, with lower strain amplitudes resulting in higher initial |E*| values [4,23]. Fatigue life increases both as strain amplitude decreases and, in general, as temperature increases.

Fig. 7b shows the combined influence of temperature and strain amplitude on the phase angle during fatigue loading. Higher phase angle values are generally obtained with increasing temperature and strain amplitude. In contrast with the results of 2PB tests, clear phase angle peaks are observed from T/C tests. The peaks were more pronounced at 10°C and 20°C than at 30°C.

Fig. 7c highlights the strong influence of strain amplitude on the dissipated energy per cycle, with higher strain amplitudes producing greater dissipated energy at all investigated temperatures. However, tests performed at the same strain amplitude at different temperatures (e.g., 90, 100, and 120 µm/m) yield different dissipated energy values, since these also depend on the norm and phase angle of the complex modulus

Fig. 8 presents the evolution of the norm of the complex Poisson's ratio in Directions 2 and 3 and the mean value and phase angle of the volumetric strain for Hot 70/100 from T/C test results.

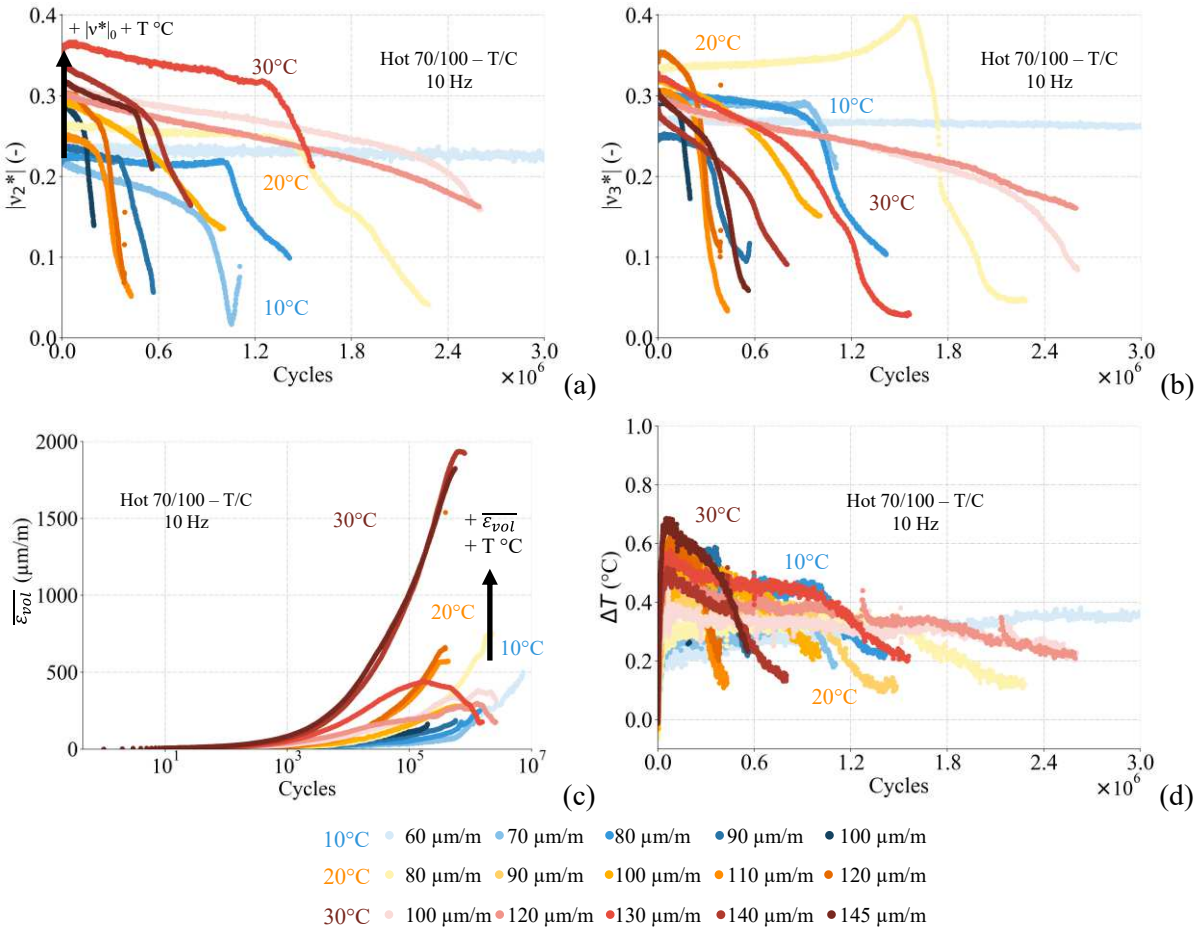


Fig. 8. Comparison of Hot 70/100 specimens tested in T/C at different strain levels at 10, 20 and 30°C: evolution with the number of loading cycles of the norm of the complex Poisson's ratio in direction 2 (a) and direction 3 (b), and mean (c) and temperature change (d).

Fig. 8a and Fig. 8b shows that higher |ν*| initial values are generally observed at higher temperatures, whereas no systematic trend with strain amplitude can be identified. During fatigue loading, the norm of the complex Poisson's ratio generally decreases with the number of cycles. However, some specimens exhibit a different evolution, including an initial increase followed by a peak, showing less consistent evolution across specimens than the complex modulus. The absence of a systematic strain-amplitude dependence is consistent with the limited sensitivity of the initial complex Poisson's ratio reported within the small-strain domain by Nguyen et al. [24]. An initial increase followed by a decrease during fatigue loading has also been reported by Tapsoba et al. [8].

Fig. 8c shows that the mean volumetric strain increases throughout fatigue loading for all specimens, indicating dilation within the instrumented region according to the adopted sign convention. In general, greater dilation is observed at higher temperatures and strain amplitudes [8,25]. Fig. 8d higher test temperatures and strain amplitudes result in both a greater temperature increases and greater volumetric dilation. Temperature dilatation of the binder may explain in part the observed variation in mean volumetric strain.

The same analysis was applied to Warm Bio using the T/C configuration. Tests were conducted at 10°C and 20°C using five strain amplitudes, with one specimen tested at each strain level. Fig. 9 presents

the evolution of the norm and phase angle of the complex modulus and the dissipated energy with the number of loading cycles for the investigated conditions.

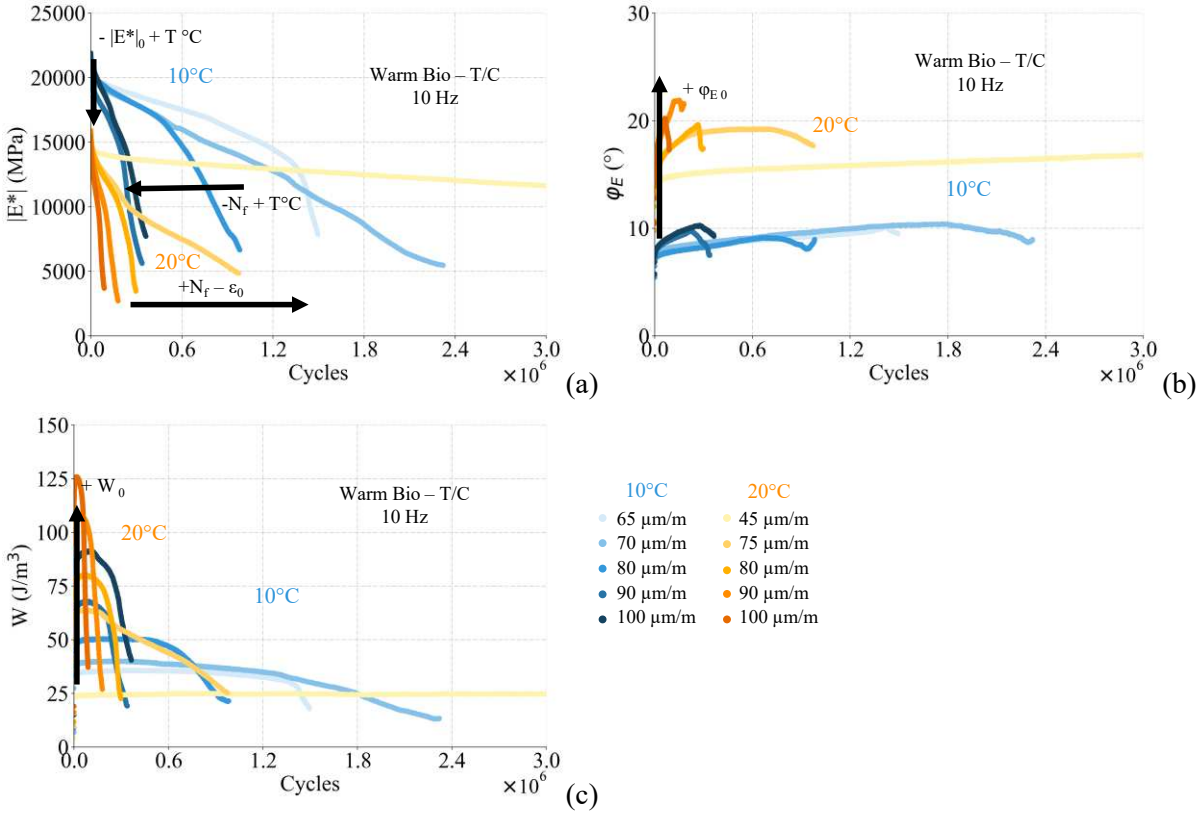


Fig. 9. Comparison of Warm Bio specimens tested in T/C at different strain levels at 10 and 20°C: evolution with the number of loading cycles of norm (a) and phase angle (b) of complex modulus and dissipated energy per cycle (c).

Fig. 9a shows a clear decrease in the initial norm of the complex modulus of Warm Bio as temperature increases. Unlike Hot 70/100, specimens tested at 20 °C generally exhibit shorter fatigue lives than those tested at 10 °C. The testing timelines were comparable between the two temperature groups, and the approximately 1 percentage point difference in air-void content is not considered sufficient to fully explain the observed reduction in fatigue life at 20 °C.

Fig. 9b shows the evolution of the phase angle of the complex modulus. Higher phase-angle values are observed at 20 °C. The occurrence of these peaks also shifts toward lower numbers of loading cycles at the higher temperature, consistently with the shorter fatigue lives observed from the modulus evolution. Fig. 9c shows that the dissipated energy per cycle increases with both temperature and strain amplitude.

Fig. 10 presents the evolution of the norm of the complex Poisson's ratio in Directions 2 and 3 and the mean value and phase angle of the volumetric strain were analyzed for Warm Bio using the T/C test results.

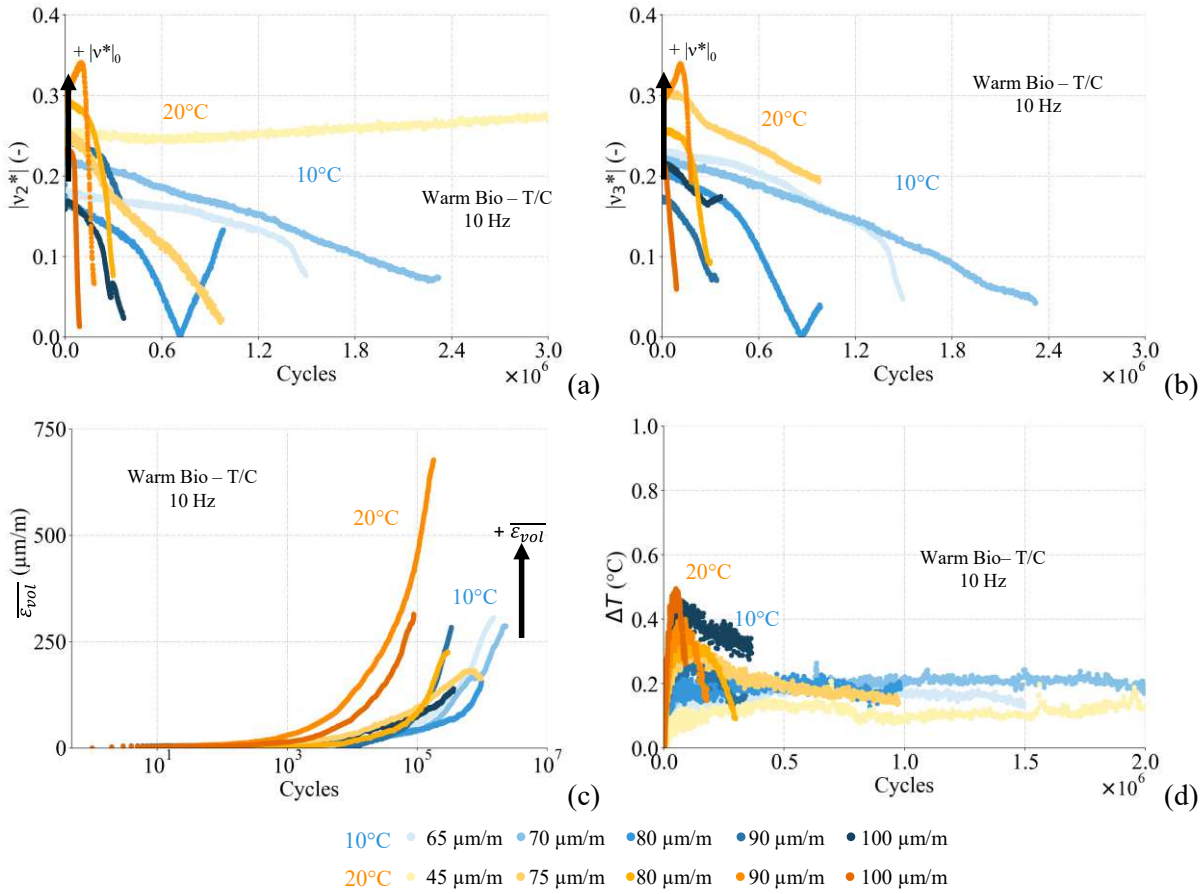


Fig. 10. Comparison of Warm Bio specimens tested in T/C at different strain levels at 10 and 20°C: evolution with the number of loading cycles of the norm of the complex Poisson's ratio in direction 2 (a) and direction 3(b), and mean (c) and temperature change (d).

Fig. 10a and Fig. 10b shows that higher |ν*| initial values are generally observed at 20 °C in both directions, while no systematic relationship with strain amplitude is identified. During fatigue loading, the norm of the complex Poisson's ratio generally decreases with the number of cycles. However, some specimens exhibit a different evolution, including an initial increase followed by a peak, confirming the relatively high variability of this parameter.

Fig. 10c shows an increase in mean volumetric strain for all Warm Bio specimens, indicating dilation of the measured specimen volume according to the adopted sign convention. In general, greater dilation is observed at higher temperatures and strain amplitudes. Fig. 10d shows that, Warm Bio exhibits similar trends as Hot 70/100, with greater heating and dilation generally observed at higher temperatures and strain amplitudes. Temperature dilatation of the binder may explain in part the observed variation in mean volumetric strain.

3.1.3 Assessment of fatigue life

The Wöhler curves obtained for Hot 70/100 using the 2PB and T/C configurations are compared in Fig. 11. T/C tests yielded shorter fatigue lives than 2PB tests at the common temperatures of 10°C and 20°C. Differences in fatigue-life estimates between testing procedures have also been reported in interlaboratory investigations [1,26]. Although the two configurations were tested at different loading frequencies and are therefore not strictly equivalent, the observed differences are also likely related to the distinct strain

definitions and stress–strain fields: 2PB uses a calculated maximum local strain in a non-homogeneous field, whereas T/C uses strain measured directly within an approximately homogeneous central region.

Consistently, the ε_6 values obtained in T/C are lower by 31 µm/m at 10 °C and 39 µm/m at 20 °C. In contrast, the slopes of the Wöhler curve, 1/b, remain comparable between configurations, with no systematic difference at the common test temperatures. The lower and upper limits of ε_6 were obtained by constructing a 95% confidence band for the regression using the Working-Hotelling method [27].

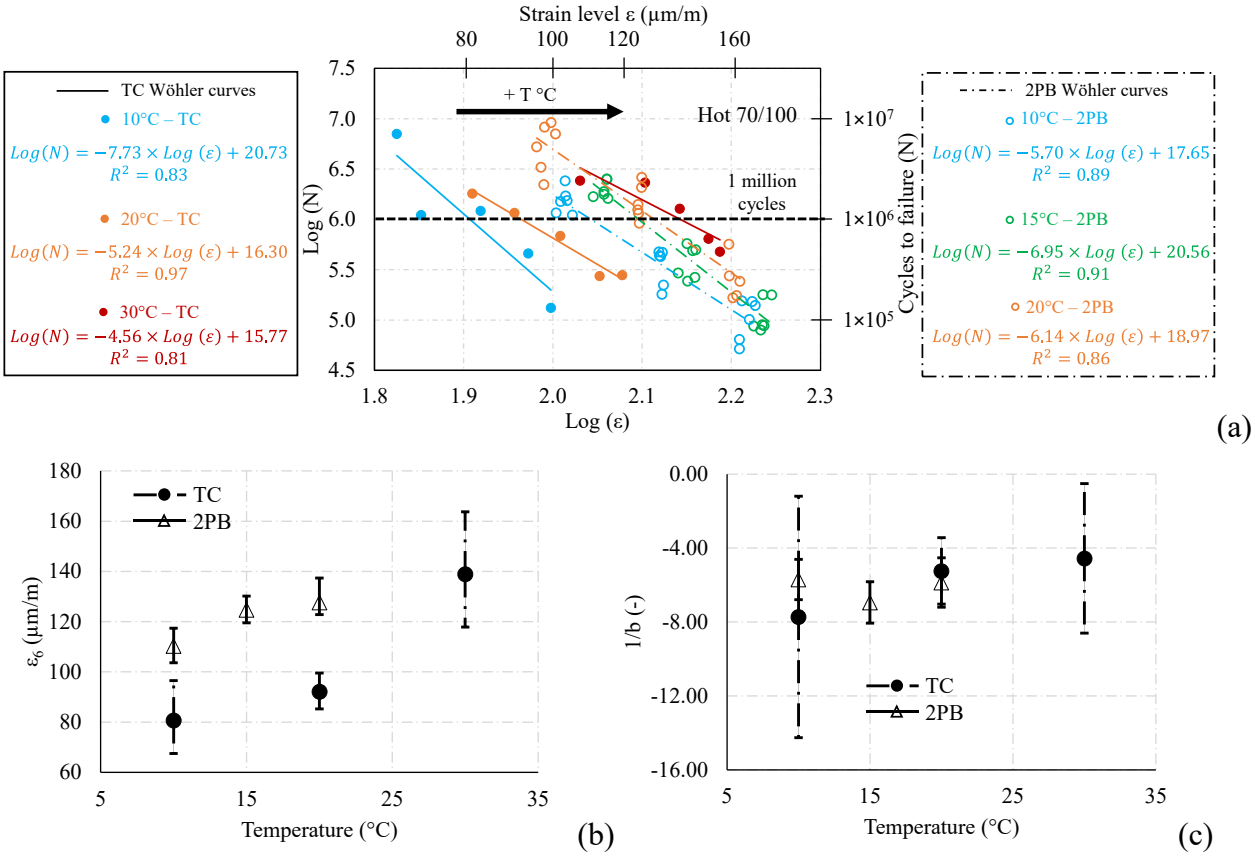


Fig. 11. Results of Hot 70/100 in 2PB and T/C at different temperatures: Wöhler curves (a) and fatigue parameters ε_6 (b) and 1/b (c).

Table 3. Summary of fatigue parameters ε_6 and 1/b of Hot 70/100 in 2PB and T/C at different temperatures.

	2PB			T/C		
Temperature	10°C	15°C	20°C	10°C	20°C	30°C
ε_6 (µm/m)	110	125	128	81	92	139
1/b (-)	-5.70	-6.95	-5.86	-7.73	-5.24	-4.56

Table 3 summarizes the fatigue parameters (ε_6) and (1/b) obtained for Hot 70/100 in both the 2PB and T/C configurations. The Wöhler curves obtained for Warm Bio using the 2PB and T/C configurations are compared in Fig. 12. For Warm Bio, no consistent temperature-related trend in (ε_6) was observed. T/C tests produced markedly shorter fatigue lives than 2PB tests at the common temperatures of 10°C and 20°C. Consistently, the ε_6 values obtained in T/C were 20 µm/m lower at 10 °C and 27 µm/m lower at 20 °C. As previously discussed, these differences may be partly related to the distinct definition and distribution of the stress and strain fields in each configuration.

It is also important to note that the 2PB tests were performed approximately one year before the T/C tests. Given the time-dependent evolution observed for Warm Bio, this difference in testing timeline may also contribute to the discrepancies between configurations. The comparison should therefore be interpreted with caution, since the observed differences cannot be attributed exclusively to the test configuration. In contrast, the Wöhler curve slopes, (1/b), remained comparable between the two configurations, with no systematic difference at the common test temperatures. The corresponding fatigue parameters ε_6 and 1/b for both configurations are summarized in Table 4.

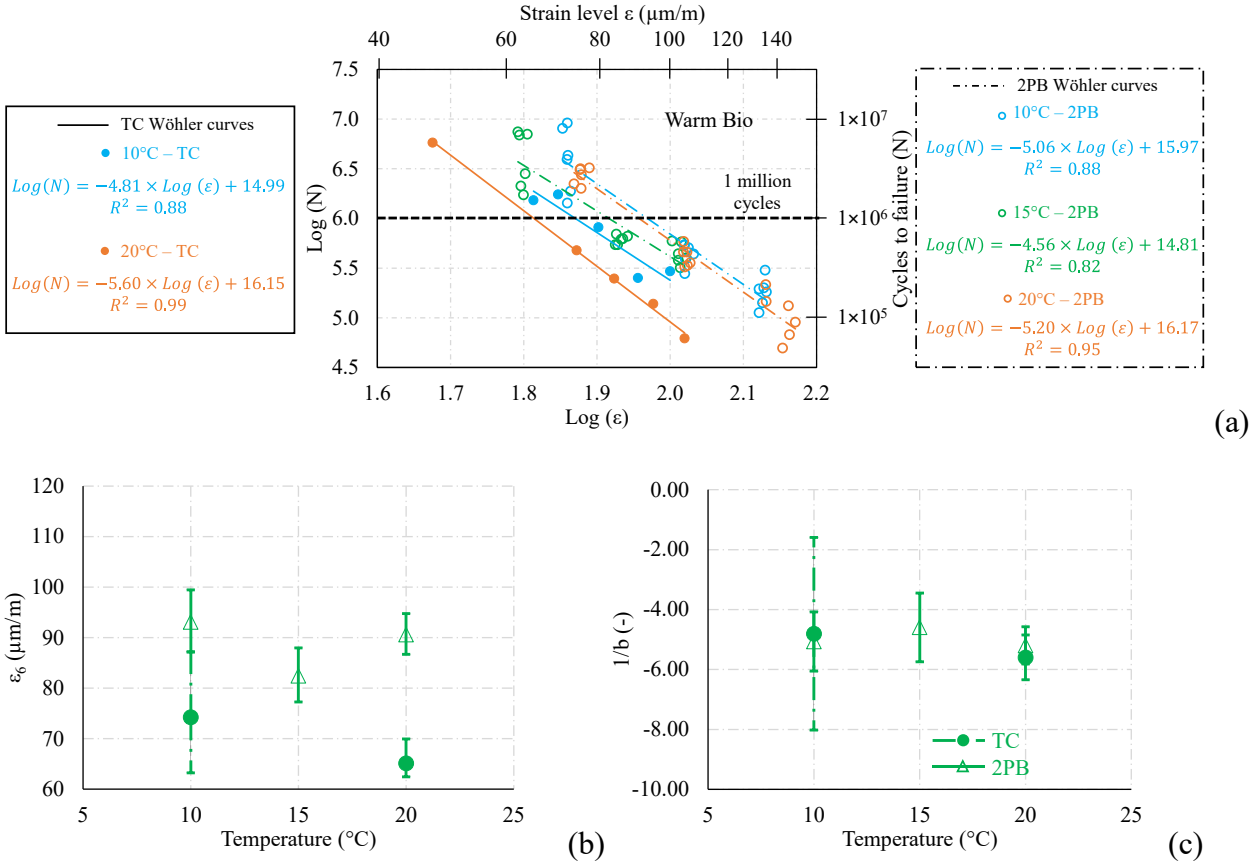


Fig. 12. Results of Warm Bio in 2PB and T/C at different temperatures: Wöhler curves (a) and fatigue parameters ε_6 (b) and 1/b (c).

Table 4. Summary of fatigue parameters ε_6 and 1/b of Warm Bio in 2PB and T/C at different temperatures.

	2PB			T/C	
Temperature	10°C	15°C	20°C	10°C	20°C
ε_6 (µm/m)	93	83	91	74	65
1/b (-)	-5.06	-4.60	-5.20	-4.81	-5.60

3.2 Influence of saturation protocol

The effect of the saturation protocol was evaluated for Hot 70/100 using 2PB tests at 10 °C. Three strain amplitudes were considered, with six specimens tested at each level, for a total of 18 specimens. Only the classical criterion based on a 50% reduction in the initial complex modulus could be evaluated, since the

tests were terminated shortly after this threshold was reached. The corresponding Wöhler curves are presented in Fig. 13.

No relevant differences in fatigue life were observed between specimens having or not withstood the saturation protocol. At 100 µm/m, saturated specimens showed longer fatigue lives, although the two groups had comparable air-void contents, differing by approximately 0.5 percentage points on average. However, this isolated difference cannot be clearly separated from specimen-to-specimen variability. The resulting fatigue parameters, ε_6 and 1/b, are presented in Fig. 14 and summarized in Table 5. No relevant difference was found for ε_6. Overall, the saturation protocol did not produce a non-negligible effect on the fatigue behavior of Hot 70/100 under the investigated conditions.

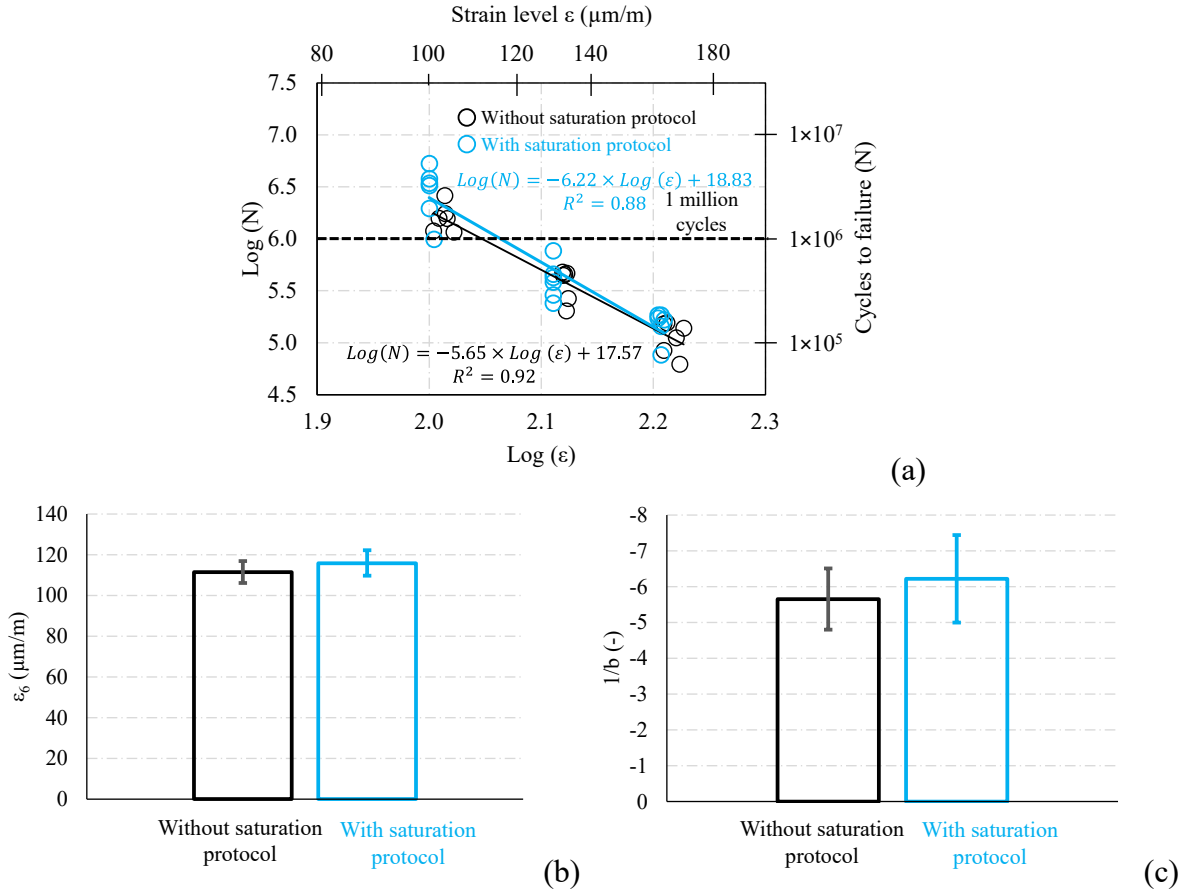


Fig. 13. Results of Hot 70/100 with and without saturation protocol in 2PB at 10°C: Wöhler curves (a) and fatigue parameters ε_6 (b) and 1/b (c).

The effect of the saturation protocol on Warm Bio is shown in Fig. 14 through the corresponding Wöhler curves. Specimens subjected to the protocol exhibited longer fatigue lives across the investigated strain amplitudes, resulting in a higher ε_6 value, while the 1/b values remained comparable.

However, this difference cannot be attributed exclusively to the saturation protocol. The specimens subjected to saturation were tested approximately one year after fabrication, whereas those tested without the protocol were evaluated less than one month after fabrication. This substantial difference in testing timeline introduces an additional variable that may have influenced the observed fatigue response. Therefore, the effect of storage time between fabrication and testing must be examined separately before the apparent improvement can be associated with the saturation protocol. This influence is investigated in

the following section. Table 5 summarizes the fatigue parameters ε_6 and 1/b of HM-70/100 in 2PB configuration comparing specimens with and without saturation protocol.

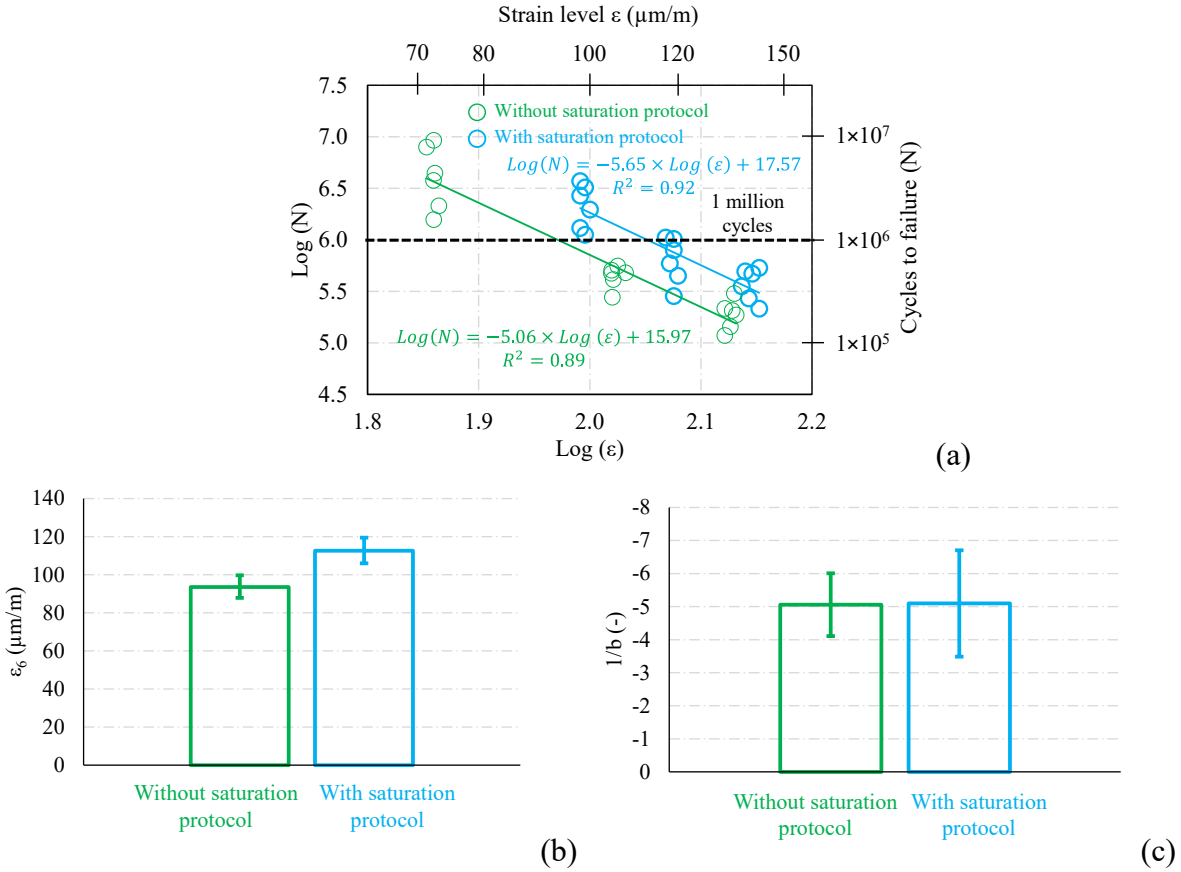


Fig. 14. Results of Warm Bio with and without saturation protocol in 2PB at 10°C: Wöhler curves (a) and fatigue parameters ε_6 (b) and 1/b (c).

Table 5. Summary of fatigue parameters ε_6 and 1/b of Hot 70/100 and Warm Bio in 2PB and T/C at 10°C.

	Hot 70/100		Warm Bio	
Saturation protocol	With	Without	With	Without
ε_6 (µm/m)	116	111	113	94
1/b (-)	-6.22	-5.65	-5.10	-5.06

3.3 Influence of storage time after fabrication

The effect of storage time was evaluated for Hot 70/100 using 2PB tests at 10 °C and a target strain amplitude of 92 µm/m. Hot 70/100 was tested at a strain amplitude close to the ε_6 value of Warm Bio-binder at 10°C and 25 Hz to assess whether it would also reach one million loading cycles at this amplitude. Six specimens from the same slab were tested at each of the three storage times, for a total of 18 specimens. Only the classical criterion based on a 50% reduction in the initial complex modulus ($N_{f\,50\%}$) could be evaluated, since the tests were terminated shortly after this threshold was reached. Fig. 15 presents the values of initial norm and phase angle of the complex modulus, together with the fatigue life, as functions of storage time after fabrication.

A slight increase in the initial norm of the complex modulus is observed with storage time, with a fitted slope of 3.69 MPa/day. However, considering the variability among specimens, this evolution remains limited. The approximately constant phase-angle values further suggest only minor rheological changes over the investigated period. Fatigue life shows substantial dispersion, and although the fitted regression indicates a decrease of approximately 1,429 cycles/day, this variation is small relative to fatigue lives on the order of (2×10^6) cycles. Overall, no clear storage-time effect can be identified for Hot 70/100 under the investigated conditions.

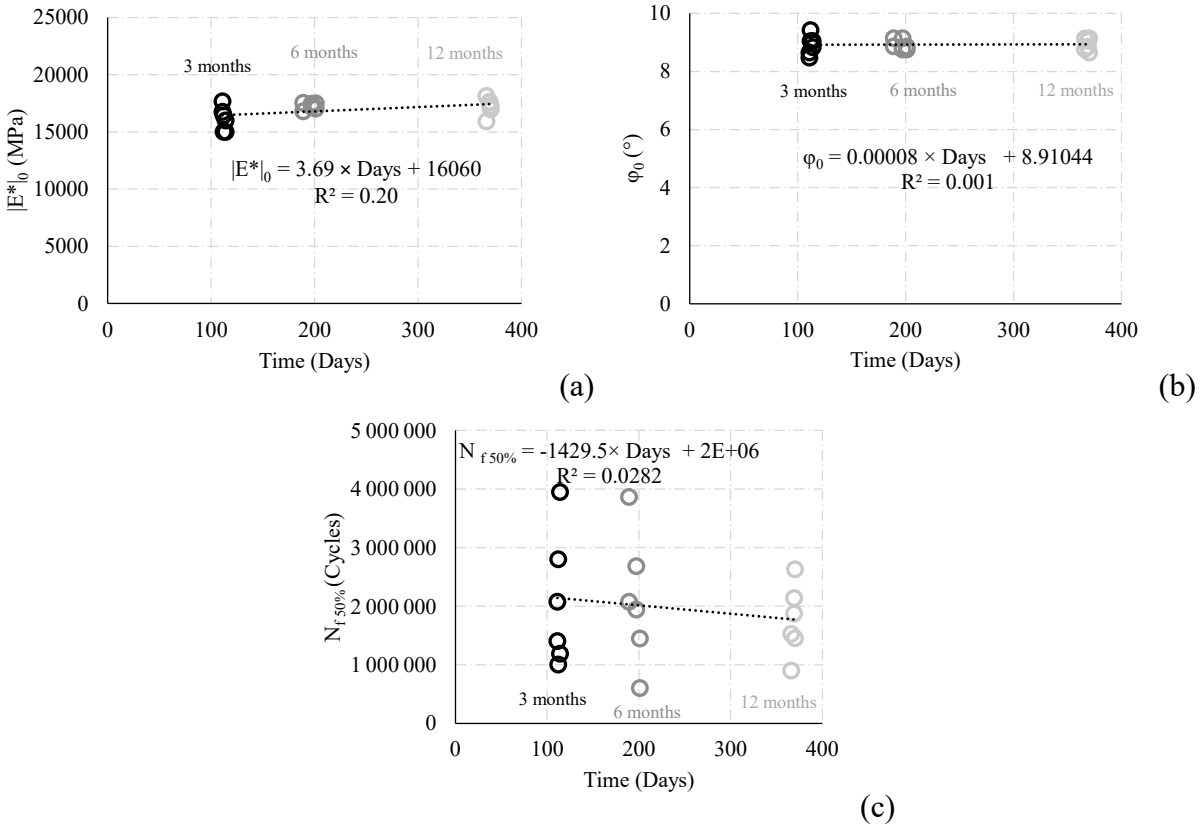


Fig. 15. Results of Hot 70/100 at different storage times in 2PB at 10°C: evolution with storage days of Initial norm (a) and phase angle (b) of the complex modulus, and fatigue life (c).

The effect of storage time was evaluated for Warm Bio using 2PB tests at 10 °C and a target strain amplitude of 109 µm/m. Warm Bio was tested at a strain amplitude close to the ε_6 value of Hot 70/100 at 10°C and 25 Hz to assess whether it would also reach one million loading cycles at this amplitude. Six specimens from the same slab were tested at each of the three storage times, for a total of 18 specimens. Fig. 16 presents the initial norm and phase angle of the complex modulus, together with the fatigue life as functions of storage time after fabrication.

The initial norm of the complex modulus increases with storage time, with a fitted slope of 9.43 MPa/day, approximately three times that the one obtained for Hot 70/100. The phase angle also decreases markedly with time, at approximately 0.0116°/day, indicating a substantially greater rheological evolution than that observed for the conventional mixture.

Despite the dispersion in fatigue life, a clear increasing trend is observed with storage time, with a fitted slope of approximately 2,275 cycles/day. After 12 months, the mean fatigue life reached

approximately (8.8×10^5) cycles. Since the applied strain amplitude of 109 µm/m is close to the ε_6 value obtained for Hot 70/100 at 10 °C, these results indicate that the fatigue performance of Warm Bio progressively approaches that of the conventional mixture over time. This pronounced evolution confirms that the storage time between fabrication and testing is a critical variable when characterizing and comparing the fatigue behavior of Warm Bio.

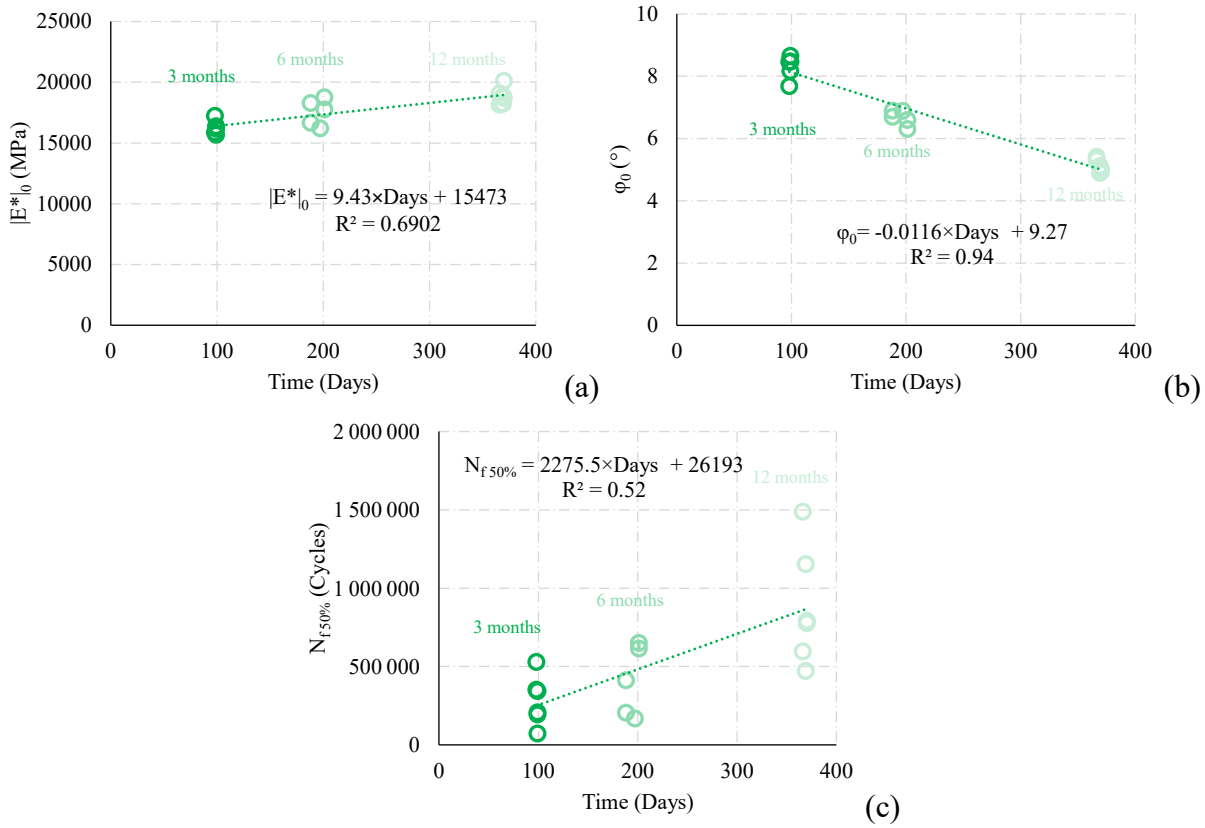


Fig. 16. Results of Warm Bio at different storage times in 2PB at 10°C: evolution with storage days of Initial norm (a) and phase angle (b) of the complex modulus, and fatigue life (c).

4. Conclusions

This study investigated the fatigue behavior of Hot 70/100 and Warm Bio using two-point bending (2PB) and tension/compression (T/C) configurations under different temperatures, strain amplitudes, conditioning states, and storage times after fabrication.

Hot 70/100 generally exhibited improved fatigue performance as temperature increased under strain-controlled loading. In both 2PB and T/C configurations, higher temperatures were associated with lower initial complex modulus, higher phase angle, and, overall, longer fatigue lives. In contrast, Warm Bio did not follow the same temperature-dependent trend. In 2PB, no systematic improvement in fatigue resistance was observed with increasing temperature, while in T/C the specimens tested at 20 °C generally exhibited shorter fatigue lives than those tested at 10 °C. These results indicate that temperature effects established for conventional mixtures cannot be directly transferred to bio-binder mixtures.

The comparison between test configurations showed consistently shorter fatigue lives and lower ε_6 values in T/C than in 2PB for both materials, whereas the Wöhler curve slopes, 1/b, remained generally comparable. These differences confirm literature findings and cannot be attributed solely to material

behavior, since the two configurations involve different strain definitions, stress and strain distributions, and loading frequencies. For Warm Bio, the interpretation is further complicated by the approximately one-year difference between the 2PB and T/C testing timelines.

The DER criterion provided a useful common basis for comparing fatigue life between the two configurations. Unlike the classical 50% modulus-reduction criterion, DER identifies failure from a change in the evolution of the material response and remained applicable under conditions where the classical criterion did not necessarily coincide with the transition from Phase II to Phase III.

The complex Poisson's ratio exhibited considerable variability between specimens and radial directions, with no consistent dependence on strain amplitude. Volumetric strain measurements showed progressive dilation during fatigue loading, generally increasing with temperature and strain amplitude. These measurements provide complementary information on the three-dimensional evolution of the specimen during fatigue.

The saturation protocol did not produce a significant change in the fatigue behavior of Hot 70/100 under the investigated conditions. For Warm Bio, specimens subjected to the protocol exhibited longer fatigue lives and higher ε_6 values; however, these specimens were tested considerably later after fabrication. The effect of saturation therefore could not be separated from the effect of storage time.

Storage time after fabrication had only a limited influence on Hot 70/100, with small changes in the initial complex modulus and no clear evolution in fatigue life. Warm Bio, however, showed a pronounced time-dependent evolution. Its initial complex modulus increased, the phase angle decreased, and fatigue life increased substantially with storage time. After 12 months, its fatigue performance approached that of Hot 70/100 under comparable loading conditions.

Overall, the fatigue response of Warm Bio is strongly influenced not only by temperature and loading conditions but also by the time storage between fabrication and testing. Specimen preparation, storage, and testing timelines must therefore be considered as critical experimental variables when characterizing and comparing bio-binder mixtures. This time-dependent evolution also highlights the need for caution when directly comparing bio-binder and conventional mixtures tested at different ages.

Statements and Declarations

Funding

This work was carried out within the framework of the CIRCOPAV project (Circular and Connected Pavements for Carbon-Neutral and Digital Roads), which has received funding from the European Union's Horizon Europe research and innovation program under the Marie Skłodowska-Curie Grant Agreement No. 101072820.

Funded by the European Union. Views and opinions expressed are, however, those of the authors only and do not necessarily reflect those of the European Union or Marie Skłodowska-Curie. Neither the European Union nor the granting authority can be held responsible for them.

Competing interests

The authors declare that they have no competing interests.

Data availability

The data that support the findings of this study are available from the corresponding author upon reasonable request.

References

[1] Di Benedetto, H., Roche, C., Baaj, H., Pronk, A., & Lundström, R. (2004). Fatigue of bituminous mixtures. Materials and Structures, 37, 202–216. https://doi.org/10.1007/BF02481620

[2] Lundström R, Di Benedetto H, Isacsson U (2004) Influence of asphalt mixture stiffness on fatigue failure. J Mater Civ Eng 16:516–525. https://doi.org/10.1061/(ASCE)0899-1561(2004)16:6(516)

[3] Boussabnia MM, Perraton D, Lamothe S, Di Benedetto H, Proteau M, Pouteau B (2023) Temperature effect on fatigue behavior of high-modulus asphalt concrete (HMAC). Constr Build Mater 409:134006. https://doi.org/10.1016/j.conbuildmat.2023.134006

[4] Mangiafico S, Sauzéat C, Di Benedetto H, Pouget S, Olard F, Planque L (2015) Quantification of biasing effects during fatigue tests on asphalt mixes: non-linearity, self-heating and thixotropy. Road Mater Pavement Des 16(sup2):73–99. https://doi.org/10.1080/14680629.2015.1077000

[5] Minhoto MJC, Pais JC, Fontes LPTL (2009) Evaluation of fatigue performance at different temperatures. In: Pais JC (ed) Proceedings of the Second Workshop on Four-point Bending. University of Minho, Guimarães, pp 217–229.

[6] Soltani A, Anderson DA (2005) New test protocol to measure fatigue damage in asphalt mixtures. Road Mater Pavement Des 6:485–514. https://doi.org/10.1080/14680629.2005.9690017

[7] Bodin D, de La Roche C, Pijaudier-Cabot G (2006) Size effect regarding fatigue evaluation of asphalt mixtures: laboratory cantilever bending tests. Road Mater Pavement Des 7(sup1):181–200. https://doi.org/10.1080/14680629.2006.9690064

[8] Tapsoba N, Sauzéat C, Di Benedetto H (2013) Analysis of fatigue test for bituminous mixtures. J Mater Civ Eng 25:701–710. https://doi.org/10.1061/(ASCE)MT.1943-5533.0000636

[9] Maggiore C, Grenfell J, Airey G, Collop AC (2012) Evaluation of fatigue life using dissipated energy methods. In: Scarpas A, Kringos N, Al-Qadi IL, Loizos A (eds) 7th RILEM International Conference on Cracking in Pavements. RILEM Bookseries, vol 4. Springer, Dordrecht, pp 643–652. https://doi.org/10.1007/978-94-007-4566-7_63

[10] Al-Khateeb GG, Alattieh SA, Zeiada W, Castorena C (2024) State-of-the-art review on the behavior of bio-asphalt binders and mixtures. Molecules 29:3835. https://doi.org/10.3390/molecules29163835

[11] Van Rompu J, Olard F, Pouget S, Schrevel F, Geisler F (2023) Mechanical and environmental performances of warm mix asphalt with reclaimed asphalt and plant-based binder. J Test Eval 51:2107–2119. https://doi.org/10.1520/JTE20220319

[12] Samieadel A, Schimmel K, Fini EH (2018) Comparative life cycle assessment (LCA) of bio-modified binder and conventional asphalt binder. Clean Technol Environ Policy 20:191–200. https://doi.org/10.1007/s10098-017-1467-1

[13] Vassaux S, Havel M, Lesueur D, Van Rompu J, Geisler F, Pouget S (2023) Development of a novel infrared methodology to assess the degree of blending in cold and warm recycled asphalt mixtures incorporating a bituminous or bio-based virgin binder. Constr Build Mater 403:133103. https://doi.org/10.1016/j.conbuildmat.2023.133103

[14] Pouget S, Loup F (2013) Thermo-mechanical behaviour of mixtures containing bio-binders. Road Mater Pavement Des 14(sup1):212–226. https://doi.org/10.1080/14680629.2013.774758

[15] Gaudenzi E, Ingrassia LP, Cardone F, Lu X, Canestrari F (2023) Investigation of unaged and long-term aged bio-based asphalt mixtures containing lignin according to the VECD theory. Mater Struct 56:82. https://doi.org/10.1617/s11527-023-02160-6

[16] Ingrassia LP, Canestrari F (2022) VECD analysis to investigate the performance of long-term aged bio-asphalt mixtures compared to conventional asphalt mixtures. Road Mater Pavement Des 23:2697–2712. https://doi.org/10.1080/14680629.2021.1991839

[17] Zhu J, Ahmed A, Dinegdae Y, Waldemarson A, Lu X, Witkiewicz P, Olsson K (2025) Long-term performance of asphalt mixtures containing bio-extended bituminous binders: laboratory investigation and accelerated pavement testing. Road Mater Pavement Des 26(sup1):135–152. https://doi.org/10.1080/14680629.2025.2482845

[18] AFNOR (2025) NF EN 12697-35: Mélanges bitumineux — Méthodes d'essai — Partie 35: Malaxage en laboratoire. AFNOR, La Plaine Saint-Denis.

[19] AFNOR (2022) NF EN 12697-33+A1: Mélanges bitumineux — Méthodes d'essai — Partie 33: Préparation de corps d'épreuve au compacteur de plaque. AFNOR, La Plaine Saint-Denis.

[20] AFNOR (2018) NF EN 12697-24: Mélanges bitumineux — Méthodes d'essai — Partie 24: Résistance à la fatigue. AFNOR, La Plaine Saint-Denis.

[21] AFNOR (2022) NF EN 12697-26+A1: Mélanges bitumineux — Méthodes d'essai — Partie 26: Rigidité. AFNOR, La Plaine Saint-Denis.

[22] AFNOR (2018) NF EN 12697-12: Mélanges bitumineux — Méthodes d'essai — Partie 12: Détermination de la sensibilité à l'eau des éprouvettes bitumineuses. AFNOR, La Plaine Saint-Denis.

[23] Nguyen QT, Di Benedetto H, Sauzéat C (2015) Linear and nonlinear viscoelastic behaviour of bituminous mixtures. Mater Struct 48:2339–2351. https://doi.org/10.1617/s11527-014-0316-5

[24] Nguyen QT, Di Benedetto H, Nguyen QP, Hoang TTN, Bui VP (2021) Effect of time–temperature, strain level and cyclic loading on the complex Poisson's ratio of asphalt mixtures. Constr Build Mater 294:123564. https://doi.org/10.1016/j.conbuildmat.2021.123564

[25] Tapsoba N, Sauzéat C, Di Benedetto H, Baaj H, Ech M (2015) Three-dimensional analysis of fatigue tests on bituminous mixtures. Fatigue Fract Eng Mater Struct 38:730–741. https://doi.org/10.1111/ffe.12278

[26] Di Benedetto, H., de La Roche, C., Baaj, H., Pronk, A., & Lundström, R. (2003). Fatigue of bituminous mixtures: different approaches and RILEM group contribution. In Proceedings of the 6th International RILEM Symposium on Performance Testing and Evaluation of Bituminous Materials (PTEBM'03) (pp. 15–38). Zurich: RILEM Publications SARL.

[27] Working, H., & Hotelling, H. (1929). Application of the theory of error to the interpretation of trends. Journal of the American Statistical Association, 24(165, Supplement), 73–85.